Stagnation point flow of Casson fluid in a porous medium with heat source/sink and inclined magnetic field

Usman Ullah[a], Salman Zeb[a,⋆], Muhammad Yousaf[a], Sardar Muhammad Hussain[b]

a. Department of Mathematics, University of Malakand, Chakdara
Dir Lower, 18800, Khyber Pakhtunkhwa, Pakistan
b. Department of Mathematical Sciences, Balochistan University of Information Technology,
Engineering and Management Sciences (BUITEMS), Quetta, 87300, Pakistan

Abstract

We analyze stagnation point flow of Casson fluid along an unsteady stretch sheet through a porous medium with impacts of inclined magnetic filed, heat source/sink, natural convection, variable heat flux, and velocity slip. The governing partial differential equations (PDEs) representing formulated fluid flow model are converted to non-linear dimensionless ordinary differential equations (ODEs) by applying similarity transformations. The ODEs solutions are evaluated numerically and the results are presented graphically showing influences of the governing parameters on velocity and temperature profiles. Enhancing behavior of the velocity profile is observed by augmenting the Grashof number and velocity ratio parameter while it is declining for magnetic parameter, unsteadiness parameter, porosity parameter, inclined angle, Casson parameter, and velocity slip parameter. The temperature profile increases by raising the magnetic parameter, inclined angle, unsteadiness parameter, porosity parameter, heat source/sink parameter, and velocity slip parameter, while it is reducing for raising values of velocity ratio parameter and Grashof number. We also showed accuracy of present results as compared with previous numerical solutions for skin friction values against unsteadiness parameter.

Keywords: Casson fluid, stagnation point, inclined magnetic field, heat source/sink, porous medium.
⋆**Corresponding author:** Salman Zeb, salmanzeb@uom.edu.pk, Tel. +92 3449220088.

1 Introduction

Significant interest in the studies of non-Newtonian fluids has been observed in the literature recently due to its increasing applications in the industry and technology. Gypsum, quicksand, paint, cream, asphalt are some examples of the non-Newtonian fluids. In these fluids, a non-linear relation exists between the shear stress and rate of deformation. The behavior of non-Newtonian fluids cannot be modeled and explained by a single constitutive equation because of its complex rheology. The primary distinctions between various non-Newtonian fluid categories can be attributed to their viscosity, a prominent physical characteristic within the boundary layer region. The nature of the boundary layer flow not only affecting the drag at a surface or on an immersed body but it also influences the heat and mass transfer rates when temperature or concentration gradients exist. Various constitutive model equations are developed by the researchers to describe the behavior of these fluids. For properties and applications of non-Newtonian fluid, we refer the readers to [1–6]. Casson fluid [7] is a non-Newtonian fluid which is viscoelastic in nature having yield stress and exhibiting shear-thinning characteristics.

It is used in many application areas such as in bio-engineering operations, food processing, biological treatments, drilling processes, and in metallurgy. Some examples of this kind of fluid in everyday life includes Jelly, toothpaste, honey, blood etc. For rheology and fluid flow behavior of viscoelastic materials, we refer to Bird et al. [8].

Casson fluid flow and heat transfer analysis with various effects has been carried out by many researchers. Mukhopadhyay et al. [9] investigated unsteady Casson fluid flow along an unsteady stretch surface and analyzed that temperature is increasing and velocity showing a declining trend for Casson fluid parameter. Magnetohydrodynamics (MHD) radiative Casson fluid flow having heat source and suction impacts with variable thermo-physical properties were elaborated by Animasaun et al. [10]. Tamoor et al. [11] analyzed flow of the viscous dissipated Casson fluid along a stretched cylinder along with magnetic field and Ohmic heating. Casson fluid behavior along a stretch sheet having effects of stagnation point, Joule heating, magnetic parameter, and viscous dissipation were inspected in [12]. Khan et al. [13] discussed unsteady Casson fluid behavior along a stretchable surface while including chemical reaction and velocity ratio parameter impacts. Analysis of Casson liquid flow with chemical reaction, magnetic parameter, and heat source/sink effects through a vertical porous surface has been studied by Vijaya and Reddy [14]. They observed that concentration distribution diminishes for chemical reaction parameter. Features of Casson nanofluid by maintaining the flow via a permeable media over a non-linear stretch sheet having impacts of slip boundary conditions and magnetic parameter were discussed by Rasool et al. [15]. They analyzed that temperature profile increases for thermophoresis and Brownian motion parameters. Analysis of radiative Casson fluid flow through an exponential stretch curved surface by considering the impacts of magnetic field, Joule heating, variable heat soruce/sink, and convective condition were carried out by Kumar et al. [16]. It was observed from their results that curvature parameter boost the velocity profile while opposite trend is depicted for Casson fluid parameter. Abo-Dahab et al. [17] inspected thermophysical properties of chemically reactive Casson nanofluid along with heat generation/absorption and suction/injection. The authors in their work [18] analyzed chemically reactive Casson fluid permeable media flow through a shrinking wall having influences of magnetic parameter and heat generation/absorption. Hussain et al. [19] scrutinized MHD radiative flow of Casson fluid with Ohmic heating along an permeable stretch wedge. Kumar et al. [20] discussed unsteady chemically reactive Casson liquid flow through a permeable vertical plate having Soret and Dufour effects and analyzed that velocity profile increases for the porosity parameter while it declines against the Casson fluid parameter. Atif et al. [21] investigated Casson fluid flow with nanoparticles having Joule heating, activation energy, convective condition, magnetic parameter, and temperature dependent thermal conductivity and viscosity along a stretchable sheet. Mahabaleshwar et al. [22] examined analytical solution of Casson nanofluid with thermal radiation through shrinking/stretching sheet with mass transpiration.

Li et al. [23] investigated activation energy impact on radiative Casson nanofluid squeezed flow in Darcy–Forchheimer permeable media with impacts of viscous dissipation, magnetic parameter, heat source/sink, and Ohmic heating. They revealed that velocity field depicted a declining trend against the Darcy–Forchheimer porosity parameters. In [24], the authors examined heat and mass transport properties of Casson liquid flow along a cylinder in a wavy channel. Malik et al. [25] explored viscous dissipated Casson fluid flow while considering the effects of heat source/sink, mixed convection, inclined magnetic field, convective and exponential thermal stratification conditions along an inclined sheet. Their analysis described that temperature field decline against thermal stratification parameter and increases for Biot number while velocity field decreases against magnetic field and inclination angle parameters. Khader et al. [26] deliberated unsteady flow of viscous dissipated Casson fluid along with magnetic field, heat source/sink, variable heat flux and velocity slip conditions by using finite element method. Nadeem et al. [27] discussed Casson nanofluid flow along a slandering surface while considering

nanofluid viscosity in the exponential form, and with Brinkman and Einstein viscosity models. Raje et al. [28] elaborated Casson fluid flow through a circular pipe while considering heat generation, porous media, magnetic field, and entropy generation influences. It was concluded from their analysis that temperature field and entropy generation enhances with raising of Casson fluid parameter while both showing a declining trend against Prandtl number. Babu [29] investigated radiative chemically reactive viscous dissipated unsteady Casson fluid flow in a permeable media along an infinite oscillating vertical plate by incorporating heat source/sink, free convection, magnetic field, and Newtonian heating. Lone et al. [30] considered MHD bio-convective chemically reactive radiative Casson nanofluid flow having influences of activation energy, and heat source along a stratified stretchable sheet and observed that velocity profile decreases with magnetic and Casson fluid parameters. They also noticed that temperature field is increasing against thermal radiation and magnetic parameters and decreases for Prandtl number and Casson fluid parameter. Mixed convective porous medium Casson fluid flow with influences of inclined magnetic field, chemical reaction, thermal radiation, Soret and Dufour effect, and suction/injection along a vertical sheet were examined by Reddy et al. [31]. Salahuddin and Awais [32] analyzed viscous dissipated radiative MHD Casson fluid with chemical reaction, activation energy, and heat generation along an upper horizontal parabolic sheet with Darcy-Forchheimer porous media and variable fluid properties by utilizing Adams-Bashforth numerical technique. They observed that concentration field decrease against activation energy and chemical reaction parameters while temperature field increases for heat source and thermal radiations. For some further interesting studies on Casson fluid flow problems, we also refer the readers to [33–38].

In this work, we consider unsteady stagnation point Casson fluid flow through an unsteady stretch surface with effects of inclined magnetic field, natural convection, and velocity slip. We also consider heat source/sink in thermal energy equation and variable heat flux at the surface. The flow is occurring in a porous medium. Governing mathematical model is developed for unsteady Casson fluid flow along an unsteady stretchable surface with considered impacts. It is then transformed to non-linear ODEs by using some similarity variables and are solved numerically. Comparison of skin friction coefficient results with previous data has been done to analyze accuracy of our results. Nusselt number and skin friction variations are analyzed against the key governing parameters. Velocity and temperature fields against the various parameters are depicted graphically and their behaviors are thoroughly explained. This work is motivated to address the following objectives.

- To analyze stagnation point flow of Casson fluid past an unsteady stretch sheet in a porous media.
- To investigate inclined magnetic field ad natural convection effect on Casson fluid flow profiles.
- What is the effect of velocity slip on stagnation point flow of Casson fluid.
- How heat source/sink influences temperature distribution and heat transfer rate.

This research study is organized as follows. In Section 2 problem formulation and conversion of PDEs to non-linear ODEs are presented. Results and discussion are presented in Section 3, and the conclusion of the work is given in Section 4.

2 Problem Formulation

We formulate Casson fluid stagnation point flow in a permeable medium along an unsteady stretched surface. The flow is assumed to be unsteady laminar incompressible and two dimensional. The sheet emerges from the slit at the origin and stretch along the x-axis at a velocity of $U(x,t) = \frac{cx}{1-\alpha t}$, with $c > 0$ and $\alpha \geq 0$. Both c and α are constants having dimensions $(s)^{-1}$, where c represents initial

stretch rate of the sheet. The sheet velocity $U(x,t)$ is applicable only for $\alpha t << 1$, i.e. $t < \frac{1}{\alpha}$ unless $\alpha = 0$. Magnetic field inclined at angle γ along x-axis and the effect of natural convection are taken in consideration, whereas the heat source/sink influence is included in heat transfer phenomena. The flow is subjected to velocity slip and variable heat flux at surface boundary, and the flow geometry is depicted in Fig. 1.

Under the aforementioned assumptions and using approximations for boundary layer, we have the following governing equations for the Casson fluid flow and heat transfer phenomena

$$\frac{\partial u}{\partial x} + \frac{\partial v}{\partial y} = 0, \tag{1}$$

$$\frac{\partial u}{\partial t} + u\frac{\partial u}{\partial x} + v\frac{\partial u}{\partial y} = U_\infty \frac{dU_\infty}{dx} + \nu\left(1+\frac{1}{\beta}\right)\frac{\partial^2 u}{\partial y^2} + \left[\frac{\sigma B_0^2}{\rho}\sin^2\gamma + \left(1+\frac{1}{\beta}\right)\frac{\nu}{K_1}\right](U_\infty - u) + g\beta_T(T - T_\infty), \tag{2}$$

$$\frac{\partial T}{\partial t} + u\frac{\partial T}{\partial x} + v\frac{\partial T}{\partial y} = \frac{\kappa}{\rho c_p}\frac{\partial^2 T}{\partial y^2} + \frac{Q_0}{\rho c_p}(T - T_\infty), \tag{3}$$

with conditions given by

$$\begin{aligned} &u = U(x,t) + N_1\left(1+\frac{1}{\beta}\right)\frac{\partial u}{\partial y}, v = 0,\ q_s(x,t) = -\kappa\frac{\partial T}{\partial y},\ \text{at } y = 0, \\ &u = U_\infty = \frac{bx}{1-\alpha t},\ T \to T_\infty,\ \text{as } y \to \infty. \end{aligned} \tag{4}$$

Here u and v are components of velocity in the x and y-axis directions respectively, $N_1 = N(1-\alpha t)^{\frac{1}{2}}$ denoting the velocity slip factor, the initial value of the velocity factor is denoted by N, x and y showing directions of the dimensional components along and perpendicular to the sheet surface, ν the kinematic viscosity, $\beta = \mu_B\sqrt{2\pi_c}/P_y$ represents the Casson parameter, B_0 the magnetic field strength, g denotes gravitational acceleration, β_T the thermal expansion coefficient, ρ is fluid density, U_∞ represents the free stream velocity, T the fluid dimensional temperature, T_∞ denoting the free stream dimensional temperature, c_p the specific heat at constant pressure, K_1 stands for permeability of porous medium, Q_0 the heat source/sink coefficient, σ is the electric conductivity of the fluid, $q_s(x,t) = -\kappa\frac{\partial T}{\partial y} = T_0\left(\frac{dx^r}{(1-\alpha t)^{m+\frac{1}{2}}}\right)$ denoting the surface heat flux, T_0 denote the reference temperature, and r and m are space and time indices, respectively.

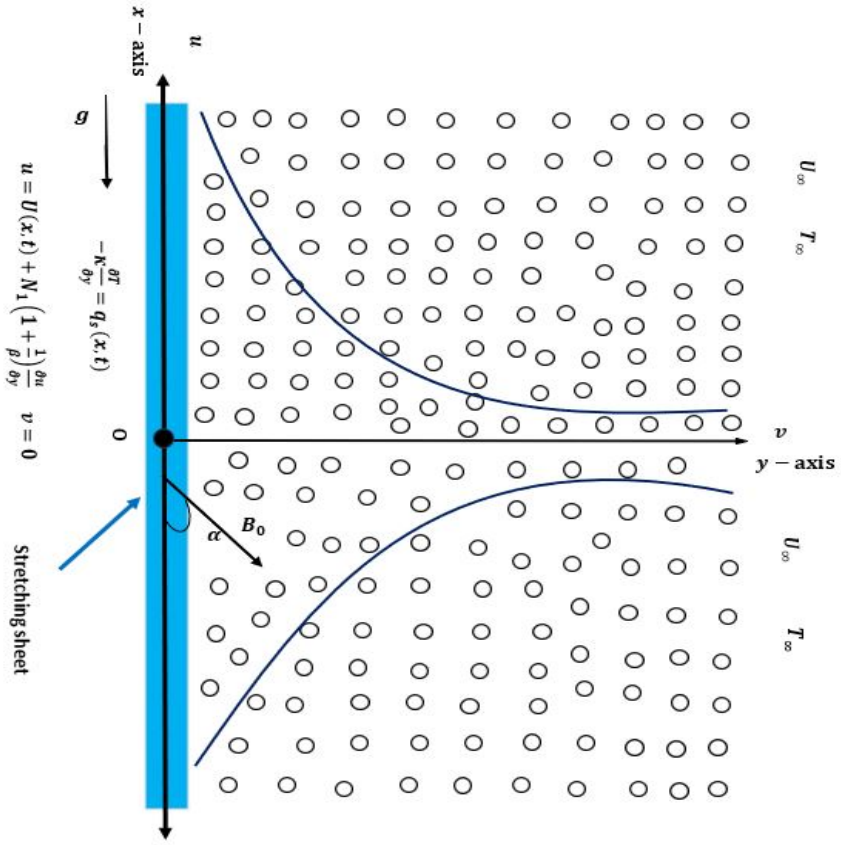

Figure 1: Model geometry

Consider the following similarity transformations

$$\eta = \left[\frac{c}{\nu(1-\alpha t)}\right]^{\frac{1}{2}} y,\ \psi = \left[\frac{\nu c}{1-\alpha t}\right]^{\frac{1}{2}} x f(\eta),\ \theta(\eta) = \frac{T - T_\infty}{T_0\left[\frac{dx^r}{\kappa\sqrt{c/\nu}}\right](1-\alpha t)^{-m}},$$
$$T = T_\infty + T_0\left[\frac{dx^r}{\kappa\sqrt{c/\nu}}\right](1-\alpha t)^{-m}\theta(\eta),\ T_w = T_\infty + T_0\left[\frac{dx^r}{\kappa\sqrt{c/\nu}}\right](1-\alpha t)^{-m}\theta(0). \tag{5}$$

where T_w is the wall temperature, ψ denoting the stream function and velocity components in terms of this are $u = \frac{\partial \psi}{\partial y}$ and $v = -\frac{\partial \psi}{\partial x}$, and $\theta(0)$ is the dimensionless sheet temperature. By substituting Eq. (5) in Eqs. (1)-(3) and in boundary conditions (4), Eq. (1) is satisfied, and further we get

$$\left(1+\frac{1}{\beta}\right)f''' + ff'' - S\left(\frac{\eta}{2}f'' + f'\right) + \left[M^2 sin^2\gamma + K\left(1+\frac{1}{\beta}\right)\right](A - f') + Gr\theta + A^2 = 0, \tag{6}$$

and

$$\theta'' + Pr\left[\left(f - \frac{\eta}{2}S\right)\theta' - \left((mS - Q) - rf'\right)\theta\right] = 0, \tag{7}$$

which are the non-linear transformed ODEs with following conditions

$$f^{'}(\eta) = 1 + \lambda\left(1 + \frac{1}{\beta}\right) f^{''}(\eta),\ f(\eta) = 0,\ \theta^{'}(\eta) = -1, \qquad \text{at}, \qquad \eta = 0,$$
$$f^{'}(\eta) = A,\ \theta^{'}(\eta) = 0, \qquad \text{as}, \qquad \eta \to \infty. \tag{8}$$

In Eqs. (6)-(8), we have $\lambda = N_1\left[\frac{c}{\nu(1-\alpha t)}\right]^{\frac{1}{2}}$ the velocity slip parameter, $K = \frac{v}{cK_1}$ denoting the porosity parameter, magnetic parameter is given by $M^2 = \frac{\sigma B_0^2}{\rho c}(1-\alpha t)$, $A = \frac{b}{c}$ velocity ratio parameter, $S = \frac{\alpha}{c}$ denotes the unsteadiness parameter, $Q = \frac{xQ_0}{U\rho c_p}$ representing the heat source/sink parameter, the Prandtl number is $Pr = \frac{\rho\nu c_p}{\kappa}$, $Gr = \frac{g\beta_T x\Delta T}{U^2}$ is the Grashof number where $\Delta T = T_0[\frac{dx^r}{\kappa\sqrt{\frac{c}{v}}}](1-\alpha t)^{-1}$.

Now considering some physical quantities of interests as follows:
Local skin friction coefficient C_{fx} given as

$$C_{fx} = \frac{2\tau_w}{\rho U^2},$$

where $\tau_w = -\left(\mu_B + \frac{p_y}{\sqrt{2\pi_c}}\right)\frac{\partial u}{\partial y}\Big|_{y=0}$ is the shear stress.
And local Nusselt number Nu_x as follows

$$Nu_x = \frac{xq_w}{\kappa(T_w - T_\infty)},$$

where $q_w = -\kappa\frac{\partial T}{\partial y}\Big|_{y=0}$ is the heat flux. The dimensionless form of these quantities using Eq. (5) are obtained as follows

$$\frac{1}{2}Re_x^{\frac{1}{2}}Cf_x = -\left(1 + \frac{1}{\beta}\right)f^{''}(0),\ Re_x^{-\frac{1}{2}}Nu_x = -\frac{\theta^{'}(0)}{\theta(0)},$$

where $Re_x = \frac{Ux}{\nu}$ is the local Reynolds number.

3 Results and Discussions

The numerical solution of the set of non-linear ODEs represented as in Eqs. (6)-(7) with boundary conditions specified in Eq. (8) are obtained by the use of Runge-Kutta-Fehlberg fourth-fifth order scheme (RKF45) along with shooting method executed in Mathematica software. We presented the numerical results of skin friction coefficient and Nusselt number in Table 1 for the key parameters arises in the transformed form of the governing model equations. It implies that skin friction increases against enhancing the parameter values S, α, M, Pr, m, K and declines for the remaining parameters. The Nusselt number enhances for the parameters Gr, Pr, A, and m while it declines for rest of the parameters. Furthermore, we examiend skin friction coefficient results against the unsteadiness parameter S while keeping other parameters constant and compared the obtained results with the previous solutions illustrated by Sharidan et al. [39], Chamakha et al. [40], Murkhopadhayay [41] and Khader [42] as specified in Table 2, thus validated the accuracy of our presented results. The behaviour of the temperature and velocity profiles versus the different governing parameters in the non-dimensional ODEs is visually shown and examined.

The behavior of velocity profiles $f'(\eta)$ against various parameters that arises in the governing model are illustrated in Figs. 2-3. In Fig. 2(a) the dimensionless velocity profile is exhibiting a declining

trend for the velocity slip parameter λ. Increasing λ diminishes the skin friction between the fluid and the stretchable surface which implies a decrease in the momentum boundary layer thickness and the velocity profile is also reduced. The influence of Grashof number Gr on the velocity profile is illustrated in Fig. 2(b). Enhancing its values decreases the viscous forces effect which implies the velocity field increases. Fig. 2(c) depicts declining behavior of $f'(\eta)$ against enhancing the porosity parameter K. The fluid velocity is declining against the Casson parameter β as depicted in Fig. 2(d). This decreasing behavior is seen because increasing β the fluid becomes more viscous and offers more resistance to the fluid motion. Fig. 3(a) depicts that $f'(\eta)$ is decreasing by enhancing the magnetic parameter M. The Lorentz force which is the resistive force is augmenting by enhancing M which reduces the motion of the fluid and hence velocity profile declined. Increasing the inclination angle γ augmenting the magnetic field strength which reduces the velocity profile as depicted in Fig. 3(b). Velocity field decreasing behavior is exhibited in Fig. 3(c) for the unsteadiness parameter S. As enhances S reduces the stretching rate and hence velocity field is declined. The velocity ratio parameter A effect on $f'(\eta)$ is plotted in Fig. 3(d). Here we see that the velocity profile is declining for the case of $A < 1$ which means when free stream velocity is less than the stretching velocity. Further, the velocity profile exhibit an increasing behavior for $A > 1$ that is when free stream velocity is greater than the stretching velocity. Also, no flow occurs near the sheet for when $A = 1$ that is when both free stream and stretching velocities are same.

Figs. 4, 5 and 6 shown the graphical results of governing parameters on temperature profile $\theta(\eta)$. Increasing M resulting in the reduction of velocity gradient and lead to the formation of the Lorentz forces which amplify the heat conduction process and a rise in temperature profile is observed as presented in Fig. 4(a). We observed from Fig. 4(b) that temperature distribution is increasing for raising the inclination angle parameter γ. Rise in the temperature profile is portrayed in Fig. 4(c) for the influence of the unsteadiness parameter S. Enhancing S reduces the stretching rate which diminishes the velocity profile and due to this an enhancement in the temperature field is seen. Augmenting the values of space index parameter r improve the temperature profile as shown in Fig. 4(d). Fig. 5(a) illustrates that rising the time index parameter m the temperature profile declines. Temperature field is declining for the velocity ratio parameter A as observed in Fig. 5(b). The stretching sheet looses more heat energy due to increase in A and hence temperature field diminishes. Raising the parameter λ enhances the temperature distribution which is illustrated in Fig. 5(c). This effect is due to the raising values of λ which enhances the force convection mechanism at the sheet and temperature profile increases. Variations in Grashof number Gr reduces $\theta(\eta)$ as depicted in Fig. 5(d). Fig. 6(a) highlights the impact of heat generation ($Q > 0$) and heat absorbtion parameter ($Q < 0$) on $\theta(\eta)$. Heat generation/absorption parameter increases the temperature profile. But for heat generation more heat is produced in the fluid as compare to heat absorption. Increasing trend of $\theta(\eta)$ versus porosity parameter K is portrayed in Fig. 6(b).

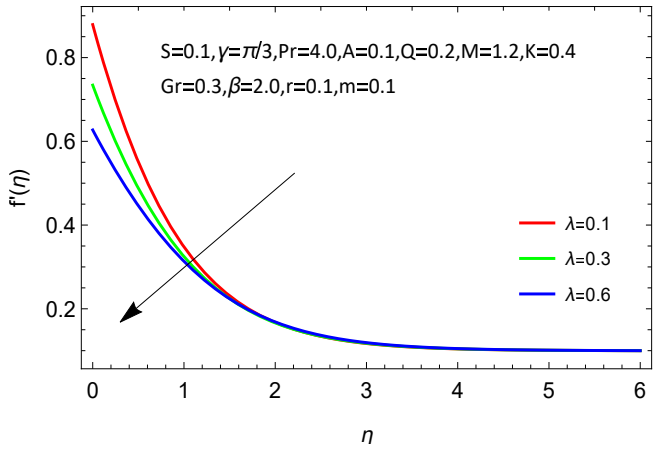

(a) $f'(\eta)$ profile for λ.

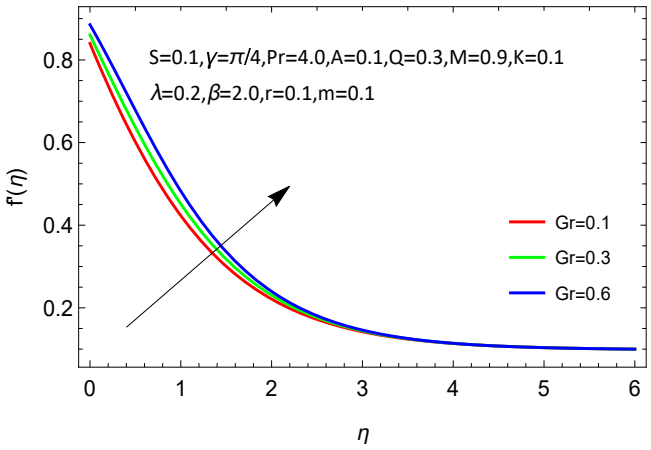

(b) Gr influence on $f'(\eta)$.

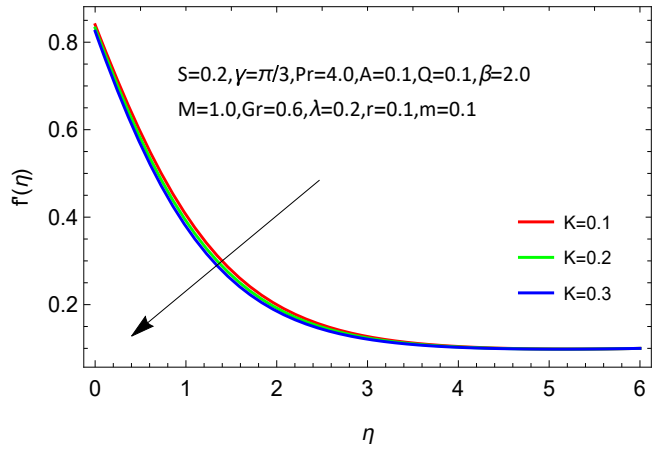

(c) K influence on $f'(\eta)$.

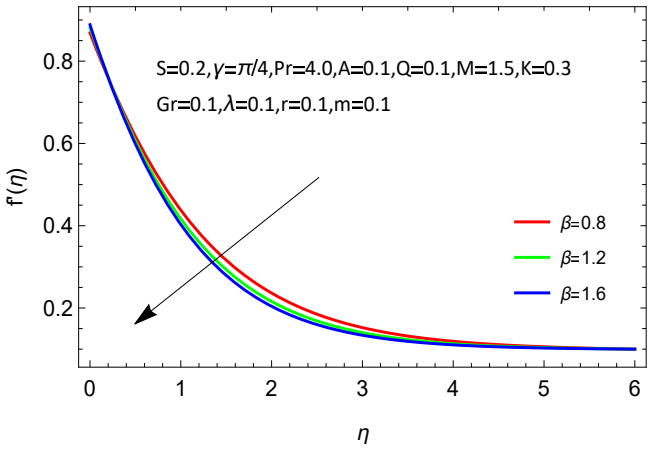

(d) β influence on $f'(\eta)$.

Figure 2: Velocity fields against λ, Gr, K, and β.

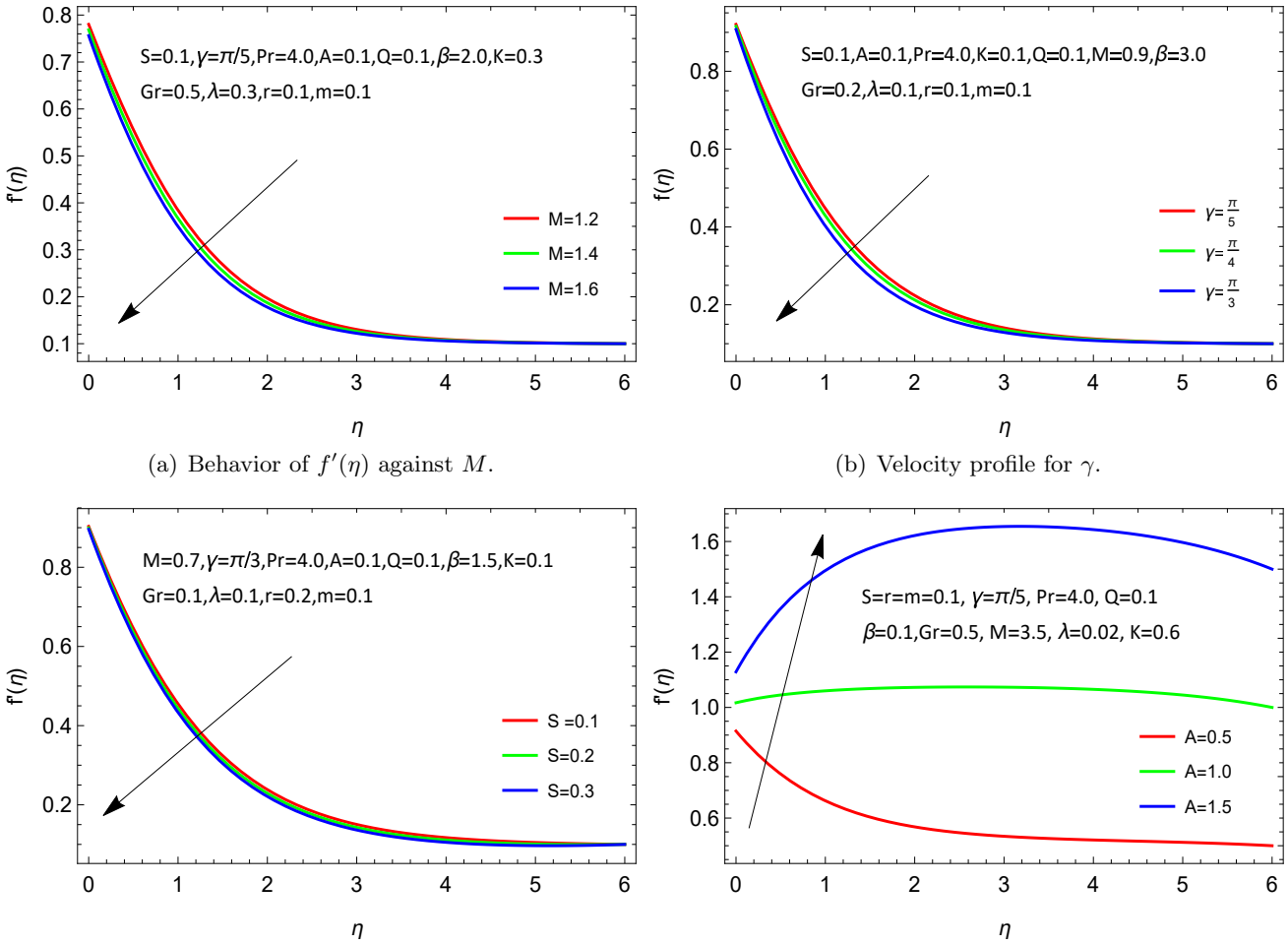

(a) Behavior of $f'(\eta)$ against M.

(b) Velocity profile for γ.

(c) S effect on $f'(\eta)$.

(d) A influence on $f'(\eta)$.

Figure 3: Velocity fields against M, γ, S, and A.

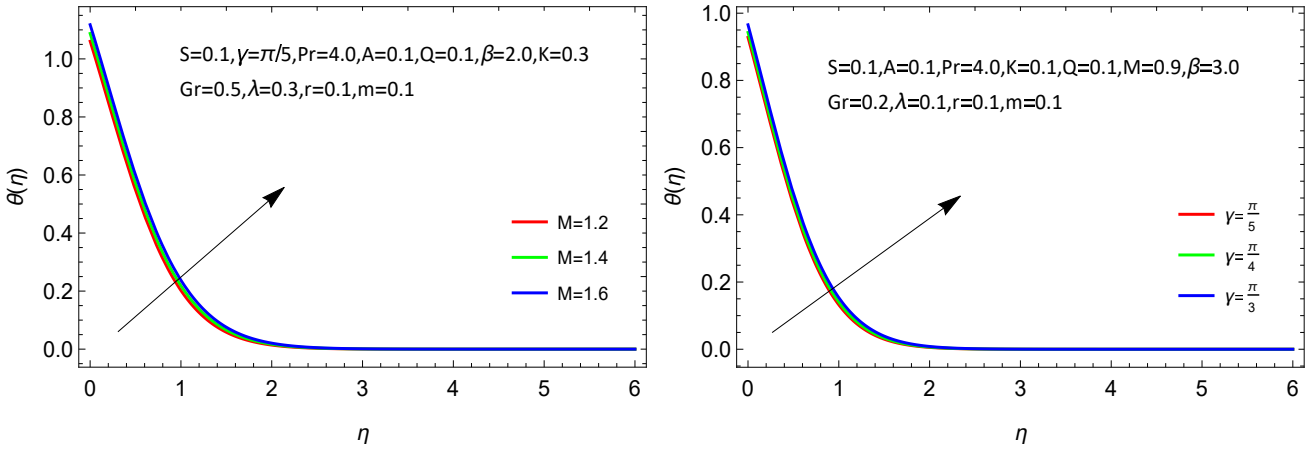

(a) Temperature distribution against M.

(b) Impact of γ parameter on $\theta(\eta)$.

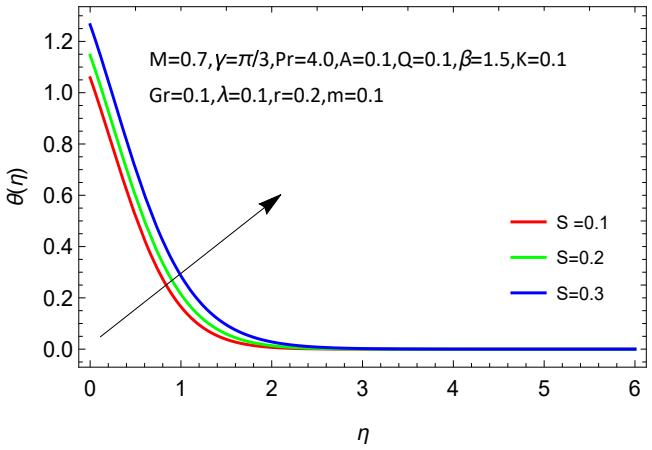

(c) $\theta(\eta)$ behavior via S.

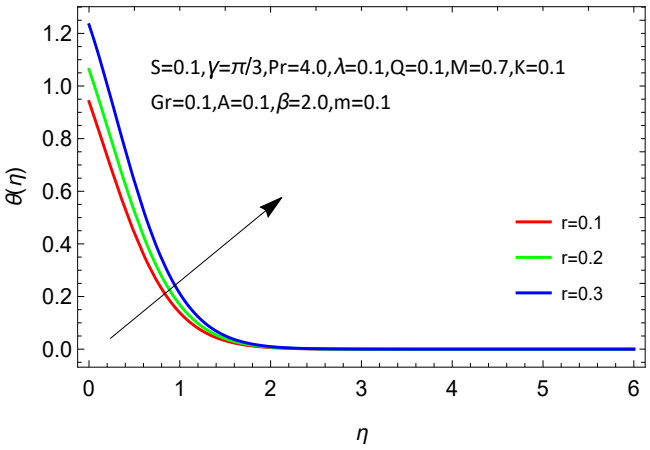

(d) $\theta(\eta)$ behavior against r parameter.

Figure 4: Temperature fields for M, γ, S, and r.

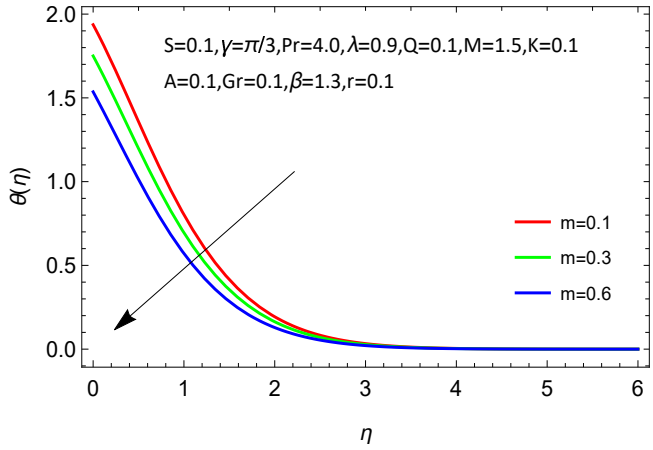

(a) $\theta(\eta)$ profile versus m.

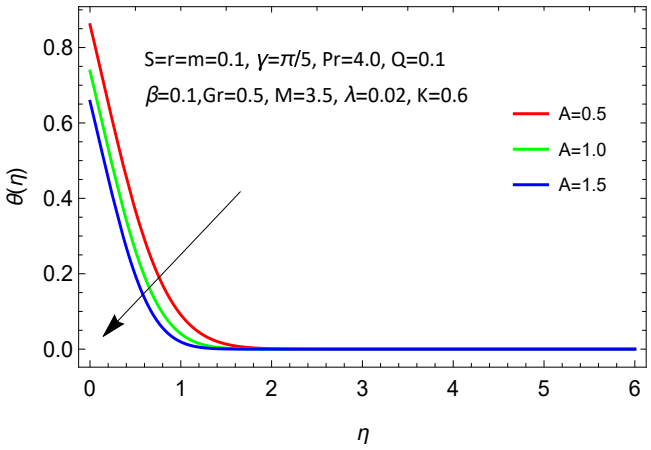

(b) $\theta(\eta)$ profile for A values.

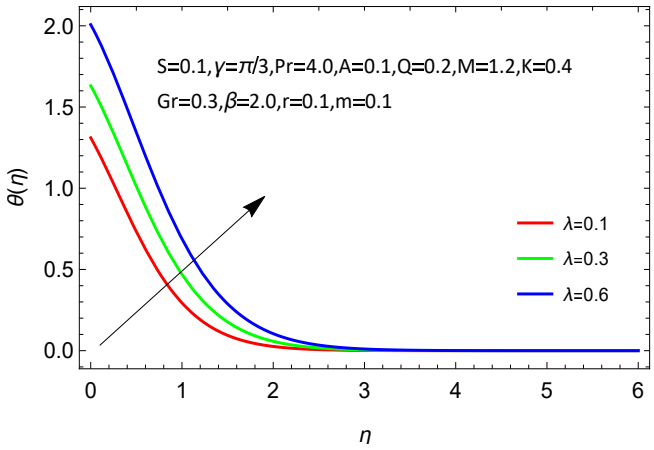

(c) $\theta(\eta)$ profile for λ values.

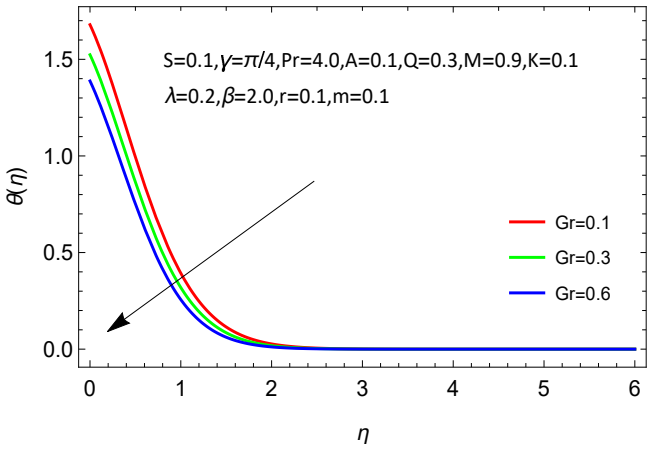

(d) $\theta(\eta)$ profile for Gr values.

Figure 5: Temperature fields for m, A, λ, and Gr.

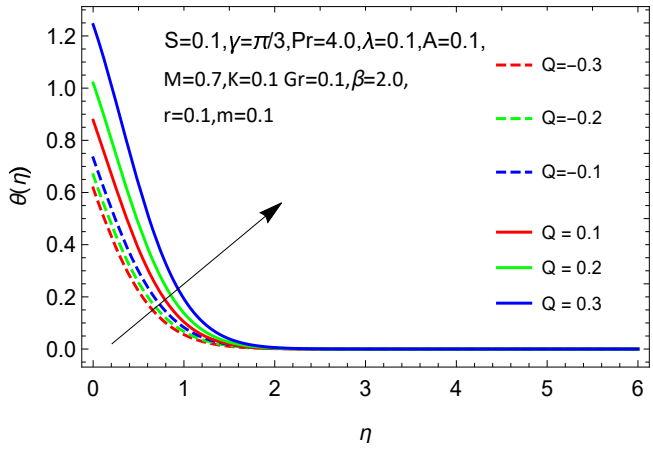

(a) $\theta(\eta)$ profile for Q values.

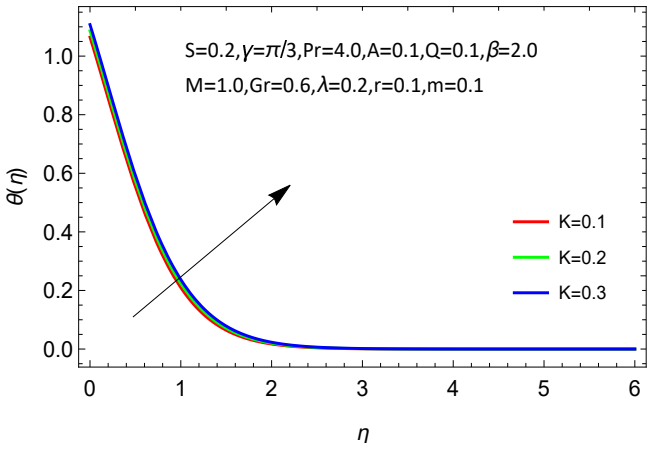

(b) $\theta(\eta)$ profile for K values.

Figure 6: Temperature fields for Q and K.

Table 1: **Skin friction coefficient and Nusselt number results for the governing parameters**

S	α	M	Gr	β	Pr	A	r	m	Q	λ	K	$-(1+1/\beta)f''(0)$	$-\theta'(0)/\theta(0)$
0.1	$\pi/4$	0.7	0.1	2.0	4.0	0.1	0.1	0.1	0.1	0.1	0.1	0.86424	1.07921
0.2												0.90627	1.01253
0.3												0.94458	0.93810
0.1	$\pi/3$	0.7	0.1	2.0	4.0	0.1	0.1	0.1	0.1	0.1	0.1	0.91943	1.06291
	$\pi/2$											0.97099	1.04745
0.1	$\pi/4$	0.8	0.1	2.0	4.0	0.1	0.1	0.1	0.1	0.1	0.1	0.89849	1.06912
		0.9										0.93558	1.05809
0.1	$\pi/4$	0.7	0.2	2.0	4.0	0.1	0.1	0.1	0.1	0.1	0.1	0.83175	1.08684
			0.3									0.80005	1.09417
0.1	$\pi/4$	0.7	0.1	2.1	4.0	0.1	0.1	0.1	0.1	0.1	0.1	0.85677	1.07860
				2.2								0.84993	1.07801
0.1	$\pi/4$	0.7	0.1	2.0	4.2	0.1	0.1	0.1	0.1	0.1	0.1	0.86588	1.11016
					4.4							0.86736	1.14038
0.1	$\pi/4$	0.7	0.1	2.0	4.0	0.2	0.1	0.1	0.1	0.1	0.1	0.74872	1.12068
						0.3						0.60140	1.16777
0.1	$\pi/4$	0.7	0.1	2.0	4.0	0.1	0.2	0.1	0.1	0.1	0.1	0.85872	0.95660
							0.3					0.85101	0.82634
0.1	$\pi/4$	0.7	0.1	2.0	4.0	0.1	0.1	0.2	0.1	0.1	0.1	0.86490	1.09544
								0.3				0.86554	1.11150
0.1	$\pi/4$	0.7	0.1	2.0	4.0	0.1	0.1	0.1	0.2	0.1	0.1	0.85566	0.90693
									0.3			0.84084	0.71322
0.1	$\pi/4$	0.7	0.1	2.0	4.0	0.1	0.1	0.1	0.1	0.2	0.1	0.77200	1.02127
										0.3		0.69828	0.97212
0.1	$\pi/4$	0.7	0.1	2.0	4.0	0.1	0.1	0.1	0.1	0.1	0.2	0.93130	1.05937
											0.3	0.99309	1.04077

Table 2: **Skin friction coefficient via unsteadiness parameter S and its comparison with previous results with $\beta \to \infty, M = K = Gr = Q = m = r = A = \lambda = 0$**

S	Results [39]	Results [40]	Results [41]	Results [42]	Present results
0.8	1.261042	1.261512	1.261479	1.26149871	1.26174
1.2	1.377722	1.378052	1.377850	1.37798514	1.37774

4 Conclusion

We investigated Casson fluid stagnation point flow in a porous medium through an unsteady stretched sheet. Inclined magnetic field, velocity slip, variable heat flux, heat source/sink, and natural convection effects are studied on the considered flow and heat transport problem. Governing PDEs representing the considered flow and heat transport phenomena are converted to non-linear ODEs via similarity

transformations. The ODEs are evaluated numerically for velocity and temperature profiles against the governing parameters. The results accuracy are validated by comparing skin friction values against the unsteadiness parameter with exsiting results in the literaure. Some important results obtained are described below.

- The velocity profile depicts an increasing behavior for enhancing the Grashof number Gr and velocity ratio parameter $A > 1$.
- Analyzing the results it is implied that fluid velocity declines due to increase in the parameters M, γ, K, S, λ, β, and for $A < 1$.
- The fluid temperature profile enhances for raising the values of M, γ, λ, S, r, K, and Q but shows reducing behavior against enhancing values of m, Gr, and A parameters.
- Skin friction increases against the higher values of S, α, M, K while it reduces for β, Gr, and A.
- The rate of heat trasnfer increases via Gr, Pr, A, and m while it decreases for rest of the parameters.

5 Disclosure Statement

The authors report there are no competing interests to declare.

Biographies

Usman Ullah has recently received his Bachelor degree in Mathematics from University of Malakand, Dir (Lower), Khyber Pakhtunkhwa, Pakistan. He has research interests in applied mathematics especially in the field of fluid mechanics.
Salman Zeb is a Lecturer in the Department of Mathematics at University of Malakand, Pakistan. His research interests include fluid mechanics, numerical analysis, and numerical solutions of differential equations. He is the author of several journal papers in these areas.
Muhammad Yousaf is an Assistant in the Department of Mathematics at University of Malakand, Pakistan. His research interests include numerical analysis, numerical linear algebra, and computational fluid dynamics.
Sardar Muhammad Hussain is an Assistant in the Department of Mathematical Sciences, Balochistan University of Information Technology, Engineering and Management Sciences (BUITEMS), Quetta, Pakistan. His research interests include hydrology, fluid mechanics, and numerical analysis.

References

[1] Barnes, H.A. "Thixotropy-A Review", *J. Nonnewton. Fluid Mech.*, **70**(1-2), pp. 1-33 (1997). https://doi.org/10.1016/S0377-0257(97)00004-9

[2] Chhabra, R.P. and Richardson, J.F. "Non-Newtonian Flow in the Process Industries: Fundamentals and Engineering Applications", 1st Edn., Butterworth-Heinemann, Oxford, UK (1999). https://doi.org/10.1016/B978-0-7506-3770-1.X5000-3

[3] Coussot, P. "Rheometry of Pastes, Suspensions, and Granular Materials: Applications in Industry and Environment", John Wiley & Sons, Inc., Hoboken, NJ, USA (2005). 10.1002/0471720577

[4] Chhabra, R.P, "Non-Newtonian Fluids: An Introduction", In Rheology of Complex Fluids, J.M. Krishnan, A.P. Deshpande, and P.B.S. Kumar, Ed., 1st Edn., pp. 3-34, Springer, New York, USA (2010). https://doi.org/10.1007/978-1-4419-6494-6

[5] Ionescu, C.M. Birs, and I.R. Copot D. et al."Mathematical modelling with experimental validation of viscoelastic properties in non-Newtonian fluids", *Philos. Trans. R. Soc. A.*, **378**(2172), 20190284, (2020). https://doi.org/10.1098/rsta.2019.0284

[6] Fagbenle, R.O. Amoo, O.M. and Falana, A. et al. "Applications of Heat, Mass and Fluid Boundary Layers", 1st Edn., Woodhead Publishing Limited, Sawston, UK (2020). https://doi.org/10.1016/C2018-0-01750-8

[7] Casson, N. "Flow equation for pigment-oil suspensions of the printing ink-type", In Rheology of Disperse Systems, C.C Mill, Ed., pp. 84-104, Pergamon Press, Oxford, UK (1959). https://api.semanticscholar.org/CorpusID:222400457

[8] Bird, R.B. Dai, G.C. and Yarusso B.J. "The rheology and flow of viscoplastic materials", *Rev. Chem. Eng.*, **1**(1), pp. 1-70, (1983). https://doi.org/10.1515/revce-1983-0102

[9] Mukhopadhyay, S. De, P.R. and Bhattacharyya, K. et al. "Casson fluid flow over an unsteady stretching surface", *Ain Shams Eng. J.*, **4**(4), pp. 933-938, (2013).https://doi.org/10.1016/j.asej.2013.04.004

[10] Animasaun, I.L. Adebile, E.A. and Fagbade, A.I. "Casson fluid flow with variable thermo-physical property along exponentially stretching sheet with suction and exponentially decaying internal heat generation using the homotopy analysis method", *J. Nigerian Math. Soc.*, **35**(1), pp. 1-17, (2016). https://doi.org/10.1016/j.jnnms.2015.02.001

[11] Tamoor, M. Waqas, M. and Khan, M.I. et al. "Magnetohydrodynamic flow of Casson fluid over a stretching cylinder", *Results Phys.*, **7**, 498-502, (2017). https://doi.org/10.1016/j.rinp.2017.01.005

[12] Nawaz, M. Naz, R. and Awais, M. "Magnetohydrodynamic axisymmetric flow of Casson fluid with variable thermal conductivity and free stream", *Alex. Eng. J.*, **57**(3), pp. 2043-2050, (2018). https://doi.org/10.1016/j.aej.2017.05.016

[13] Khan, K.A. Butt, A.R. and Raza, N. "Effects of heat and mass transfer on unsteady boundary layer flow of a chemical reacting Casson fuid", *Results Phys.*, **8**610-620, (2018). https://doi.org/10.1016/j.rinp.2017.12.080

[14] Vijaya, K. and Reddy, G.V.R. Magnetohydrodynamic "Casson fluid flow over a vertical porous plate in the presence of radiation, soret and chemical reaction effects", *J. Nanofluids*, **8**(6), pp. 1240-1248, (2019). https://doi.org/10.1166/jon.2019.1684

[15] Rasool, G. Chamkha, A.J. and Muhammad, T. et al. "Darcy-Forchheimer relation in Casson type MHD nanofluid flow over non-linear stretching surface", *Propuls. Power Res.*, **9**(2), 159-168, (2020). https://doi.org/10.1016/j.jppr.2020.04.003

[16] Kumar, K.A. Sugunamma, V. and Sandeep, N. "Effect of thermal radiation on MHD Casson fluid flow over an exponentially stretching curved sheet", *J. Therm. Anal. Calorim.*, **140**, pp. 2377-2385, (2020). https://doi.org/10.1007/s10973-019-08977-0

[17] Abo-Dahab, S.M. Abdelhafez, M.A. and Mebarek-Oudina, F. et al. "MHD Casson nanofluid flow over nonlinearly heated porous medium in presence of extending surface effect with suction/injection", *Ind. J. Phys.*, **95**, pp. 1-15, (2021). https://doi.org/10.1007/s12648-020-01923-z

[18] Awais, M. Raja, M.A.Z. Awan, S.E. et al. "Heat and mass transfer phenomenon for the dynamics of Casson fluid through porous medium over shrinking wall subject to Lorentz force and heat source/sink", *Alex. Eng. J.*, **60**(1), pp. 1355-1363, (2021). https://doi.org/10.1016/j.aej.2020.10.056

[19] Hussain, M. Ali, A. and Ghaffar, A. et al. "Flow and thermal study of MHD Casson fluid past a moving stretching porous wedge", *J. Therm. Anal. Calorim.*, **147** pp. 6959-6969, (2022). https://doi.org/10.1007/s10973-021-10983-0

[20] Kumar, M.A. Reddy, Y.D. Goud, B.S. et al. "An impact on non-Newtonian free convective MHD Casson fluid flow past a vertical porous plate in the existence of Soret, Dufour, and chemical reaction", *Int. J. Ambient Energy*, **43**(1), pp. 7410-7418, (2022). https://doi.org/10.1080/01430750.2022.2063381

[21] Atif, S.M. Shah, S. and Kamran, A. "Effect of MHD on Casson fluid with Arrhenius activation energy and variable properties", *Sci. Iran. Trans. F: Nanotech.*, **29**(6), pp. 3570-3581, (2022). https://doi.org/10.24200/sci.2021.57873.5452

[22] Mahabaleshwar, U.S. Maranna, T. and Sofos, F. "Analytical investigation of an incompressible viscous laminar Casson fluid flow past a stretching/shrinking sheet", *Sci. Rep.*, **12**(1), 18404, (2022). https://doi.org/10.1038/s41598-022-23295-6

[23] Li, S. Raghunath, K. and Alfaleh, A. et al. "Effects of activation energy and chemical reaction on unsteady MHD dissipative Darcy-Forchheimer squeezed flow of Casson fluid over horizontal channel", *Sci. Rep.*, **13**(1), 2666, (2023). https://doi.org/10.1038/s41598-023-29702-w

[24] Majeed, A.H. Mahmood, R. Shahzad, H. et al. "Heat and mass transfer characteristics in MHD Casson fluid flow over a cylinder in a wavy channel: Higher-order FEM computations", *Case Stud. Therm. Eng.*, **42**, 102730, (2023). https://doi.org/10.1016/j.csite.2023.102730

[25] Malik, H.T. Farooq, M. and Ahmad, S. et al. "Convective heat transportation in exponentially stratified Casson fluid flow over an inclined sheet with viscous dissipation", *Case Stud. Therm. Eng.*, **52**, 103720, (2023). https://doi.org/10.1016/j.csite.2023.103720

[26] Khader, M.M. Inc. M. and Akgul, A. "Numerical appraisal of the unsteady Casson fluid flow through Finite Element Method (FEM)", *Sci. Iran. Trans. B: Mech. Eng.*, **30**(2), pp. 454-463, (2023). https://doi.org/10.24200/sci.2022.60176.6644

[27] Nadeem, S. Ishtiaq, B. and Hamida, M.B.B. et al. "Reynolds nanofluid model for Casson fluid flow conveying exponential nanoparticles through a slandering sheet", *Sci. Rep.*, **13**(1), 1953, (2023). https://doi.org/10.1038/s41598-023-28515-1

[28] Raje, A. Koyani, F. and Bhise, A.A. et al. "Heat transfer and entropy optimization for unsteady MHD Casson fluid flow through a porous cylinder: Applications in nuclear reactors", *Int. J. Mod. Phys. B*, **37**(25), 2350293, (2023). https://doi.org/10.1142/S0217979223502934

[29] Babu, B.H. "Heat and mass transfer on unsteady MHD casson fluid flow past an infinite vertical porous plate with chemical reaction", *Proc. Inst. Mech. Eng. E: J. Process Mech. Eng.*, **237**(6), pp. 2278-2289, (2023). https://doi.org/10.1177/09544089221133966

[30] Lone, S.A. Anwar, S. and Saeed, A. et al. "A stratified flow of a non-newtonian Casson fluid comprising microorganisms on a stretching sheet with activation energy", *Sci. Rep.*, **13**(1), 11240, (2023). https://doi.org/10.1038/s41598-023-38260-0

[31] Reddy, B.P, Felician, A. and Matao. P.M. "Finite element simulation of Soret-Dufour and conjugate heating effects on mixed convective heat absorbing hydromagnetic Casson fluid flow with suction/blowing from at semi-infinite vertical porous plate", *Heliyon*, **10**(2), (2024) https://doi.org/10.1016/j.heliyon.2024.e24150

[32] Salahuddin, T and Awais, M. "Implementing the multistep Adams-Bashforth numerical approach on magnetohydrodynamic radiated Casson fluid with Darcy Forchheimer dissipation and activation energy", *Phys. Scr.*, **99**(2), 025224, (2024). 10.1088/1402-4896/ad190e

[33] Qasim, M. and Noreen, S. "Heat transfer in the boundary layer flow of a Casson fluid over a permeable shrinking sheet with viscous dissipation", *Eur. Phys. J. Plus*, **129**, 7, (2014). https://doi.org/10.1140/epjp/i2014-14007-5

[34] Aneja, M. Chandra, A. and Sharma, S. "Natural convection in a partially heated porous cavity to Casson fluid", *Int. Commun. Heat Mass Transf.*, **114**, 104555, (2020). https://doi.org/10.1016/j.icheatmasstransfer.2020.104555

[35] Mahabaleshwar, U.S. Mahesh, R. and Sofos, F. "Thermosolutal Marangoni convection for hybrid nanofluid models: An analytical approach", *Physics*, **5**(1), pp. 24-44, (2022). https://doi.org/10.3390/physics5010003

[36] Raje, A. and Bhise, A.A. "Heat transport in a sandwiched set-up of MHD Newtonian Casson Newtonian fluids through a porous medium", *Heat Transfer*, **52**(1), pp. 122-143, (2023). https://doi.org/10.1002/htj.22688

[37] Mahesh, R. Mahabaleshwar,U.S. and Sofos. F. "Influence of carbon nanotube suspensions on Casson fluid flow over a permeable shrinking membrane: An analytical approach", *Sci. Rep.*, **13**(1), 3369, (2023). https://doi.org/10.1038/s41598-023-30482-6

[38] Hussain, M. Shoaib, M. Ranjha, Q.A. et al. "Numerical solution to flow of Casson fluid via stretched permeable wedge with chemical reaction and mass transfer effects", *Mod. Phys. Lett. B.*, **38**(16), 2341008, (2024). https://doi.org/10.1142/S0217984923410087

[39] Sharidan, S. Mahmood, M. and Pop, I. "Similarity solutions for the unsteady boundary layer flow and heat transfer due to a stretching sheet", *Int. J. Appl. Mech. Eng.*, **11**(3), pp. 647-654, (2006). https://api.semanticscholar.org/CorpusID:119030736

[40] Chamkha, A.J. Aly, A.M. and Mansour, M.A. "Similarity solution for unsteady heat and mass transfer from a stretching surface embedded in a porous medium with suction/injection and chemical reaction effects", *Chem. Eng. Commun.*, **197**(6), pp. 846-858, (2010). https://doi.org/10.1080/00986440903359087

[41] Mukhopadhyay, S. "Effects of thermal radiation on Casson fluid flow and heat transfer over an unsteady stretching surface subjected to suction/blowing", *Chin. J. Phys.*, **22**(11), 114702, (2013). 10.1088/1674-1056/22/11/114702

[42] Khader, M.M. "Numerical study for unsteady Casson fluid flow with heat flux using a spectral collocation method", *Ind. J. Phys.*, **96**(3), pp. 777-786, (2022). https://doi.org/10.1007/s12648-021-02025-0